Use of a local-density approximation for exchange-correlation potentials in multichannel atomic quantum-defect calculations

J. A. Armstrong, Sudhanshu S. Jha,* and K. C. Pandey
IBM Thomas J. Watson Research Center, P.O. Box 218, Yorktown Heights, New York 10598
(Received 19 January 1981)

Multichannel quantum-defect theory provides an attractive framework for compact, *a priori* calculations of the binding energies or scattering resonances of highly excited, multielectron atoms. However, in addition to obtaining a good representation of interchannel interactions, it is difficult in practice to find a sufficiently accurate, self-consistent, simple, one-electron potential for describing the average motion of a Rydberg electron in the multielectron core. Moreover, when there is a nonspherical core there is a significant non-Coulomb tail even at fairly large distances from the origin, and due to exchange and correlations, such a potential will be nonlocal. We describe a self-consistent, local-density approximation to calculate a single-particle potential with proper self-interaction corrections, which represents quite accurately the motion of the outer electron in the presence of a spherically averaged core. This is derived from the well-known solid-state calculational technique based on the Hedin-Lundqvist approximation. The channel interactions and nonspherical contributions to intrachannel potentials are then calculated by explicitly considering the motion of two electrons outside the outermost closed-shell configuration of the atom. This procedure permits greatly increased accuracy in the prediction of excited-state energies of the entire spectral series. Explicit numerical results for quantum-defect parameters are presented for many Rydberg series in several alkali-metal and alkaline-earth atoms.

I. INTRODUCTION

Accurate calculations of the binding energies of the highly excited, atomic Rydberg states become very difficult within the framework of the standard configuration-interaction scheme. This is because of the rapidly increasing number of relevant configurations which must be included in such calculations. On the other hand, it is known[1] that precise binding energies of an entire series of even strongly perturbed Rydberg states may be reproduced from knowledge of a small set of parameters of the multichannel quantum-defect theory (MQDT).[2,3] Therefore, an appealing approach to accurate calculation of excited-state energies would be to calculate MQDT parameters instead. The accuracy of such an approach *improves* as one goes to higher and higher Rydberg levels.

In fact, the MQDT was developed originally[2] as a means of simplifying *a priori* calculations of electron-ion scattering cross sections and bound-state energies of Rydberg states. A number of calculations have been made, both of continuum scattering[4] and bound-state energies,[5-7] but in many cases, except for one electron outside a closed-shell core, the uncertainty of *a priori* calculations of excited-state energies has been substantial in comparison to the interval between excited states. In Ref. 8 we described briefly an MQDT calculational scheme, applied to alkaline-earth atoms, which achieved substantially improved accuracy. It is the aim of this paper to give a thorough description of this scheme so that it may be exploited and improved further by anyone interested in such calculations.

The accuracy in calculating MQDT parameters has been limited[5-7] mainly by difficulties in obtaining and using a sufficiently precise self-consistent one-electron potential seen by the Rydberg electron in the core region. When there is more than one electron outside the closed shell, the Hartree potential in general corresponds to a nonspherical charge density of the remaining core. Thus, one has still a significant contribution to the potential from non-Coulomb tails even at fairly large r. This forces us to integrate the radial Schrödinger equation, valid in the inside region of the atom, up to very large distances (15–25 a.u.) from the origin, where without much error one can assume the potential to become Coulombic $(-1/r)$ and match the solution to a linear combination of Coulomb functions[9] in the outer region. Further, one has to take account of possible strong interactions between various Rydberg channels, which differ from one another in the electronic configuration of the $(Z-1)$ core electrons and possibly also in the orbital angular momentum of the Rydberg electron. In such a case, one has to solve a coupled multichannel problem in the inside region.

However, the greatest computational difficulty arises from the nature of the exchange and correlation potential, which makes both intrachannel and interchannel interactions *nonlocal* in the inside region. This leads to the problem of solving *coupled integrodifferential* equations for the interacting channels.[7] Even for a noninteracting Rydberg channel, one has to handle an integrodif-

ferential equation, instead of an ordinary differential equation.

To simplify this problem considerably, we recently introduced a self-consistent local-density approximation for the intrachannel exchange-correlation potential to calculate[8] quantum-defect parameters in Ca, Sr, and Ba. This approximation is based on the local-density approximation of Hedin and Lundqvist,[10] widely used in solid state calculations. But unlike the case of the Hedin-Lundqvist (HL) exchange-correlation potential, which goes to zero exponentially at large distances, our self-consistent exchange-correlation potential includes the self-interaction correction, first suggested by Perdew,[11] which, as it should, exactly cancels the self-interaction term included in the Hartree potential. This means that our total intrachannel potential in a neutral atom goes over correctly to $-1/r$ (in atomic units) at large distances.

In the following sections we describe in detail how we construct our intrachannel and interchannel potentials, and how we use them to calculate quantum-defect parameters for several Rydberg channels in atoms with one or two electrons outside a closed shell. In Sec. II of the paper, we briefly review the local-density approximation of Slater[12] and of Hedin and Lundqvist[10] for obtaining a local potential beyond the Hartree approximation. We then show how to correct the Hedin-Lundqvist approximation to obtain a local potential with self-consistent self-interaction correction. Taking specific examples of atoms with one or two electrons outside the tightly bound closed shell, we describe in Sec. III the construction of both the intrachannel and interchannel potentials. In Sec. IV, we use these to calculate quantum-defect parameters for the bound Rydberg series $ns\,^2S$, $np\,^2P$, and $nd\,^2D$ of Na and K; $ms\,ns\,^3S$, $ms\,np\,^3P$, $(m-1)d\,np\,^3P$, and $ms\,nd\,^3D$ series of Mg, Ca, Sr, and Ba, and $ms\,np\,^1P$ and $(m-1)d\,np\,^1P$ series of Ca, Sr, and Ba. We discuss our results and various approximations in Sec. V. We have assumed, in writing this paper, that the reader is more familiar with MQDT than with the density-functional theory of solid-state calculations, and therefore we have emphasized in greater detail the self-consistent local-density exchange-correlation theory. For readers who are not familiar with MQDT, we recommend Ref. 3 as background.

II. SELF-CONSISTENT POTENTIAL IN A LOCAL-DENSITY APPROXIMATION WITH CORRECTIONS FOR SELF-INTERACTION TERMS

The idea of finding an effective, self-consistent, local, single-particle potential to describe the motion of an electron in an atom goes back[13] to Thomas, Fermi, Hartree, Dirac, and Slater. It is well known that even in the simplest form, in which the electronic correlations are neglected and Hartree-Fock approximation treats a single configuration, the single-particle potential is nonlocal because of the exchange interaction. Explicitly, for the N-electron atomic Hamiltonian (in atomic units)

$$H(N)=\sum_{i=1}^{N}\left(-\frac{1}{2}\nabla_i^2-\frac{Z}{r_i}\right)+\sum_{i<j}\frac{1}{|\vec{r}_i-\vec{r}_j|}\,, \tag{2.1}$$

where $Z=N$ is the nuclear charge, the Hartree-Fock equation for the ith spin orbital $u_i(\vec{r})\chi_{\lambda_i}(\vec{\sigma})$ is given by

$$-\tfrac{1}{2}\nabla^2 u_i(\vec{r})+\left(-\frac{Z}{r}+\sum_j\int d^3r'\,\frac{u_j^*(\vec{r}')u_j(\vec{r}')}{|\vec{r}-\vec{r}'|}\right)u_i(\vec{r})$$
$$-\sum_j\left(\delta_{\lambda_i,\lambda_j}\int d^3r'\,\frac{u_j^*(\vec{r}')u_i(\vec{r}')}{|\vec{r}-\vec{r}'|}\right)u_j(\vec{r})=\epsilon_i u_i(\vec{r})\,. \tag{2.2}$$

Note that at this stage, the self-interaction term (with $j=i$) in the exchange part (the last bracket on the left-hand side) exactly cancels the $j=i$ term in the Hartree part (first bracket) on the left-hand side. Thus, the summations over j can be extended to all N occupied orbitals in both the Hartree and the exchange parts. In fact, in terms of the total electronic density,

$$n(\vec{r})=\sum_j u_j^*(\vec{r})u_j(\vec{r})\,, \tag{2.3}$$

the Hartree potential

$$V_H(\vec{r})=-\frac{Z}{r}+\int d^3r'\,\frac{n(\vec{r}')}{|\vec{r}-\vec{r}'|} \tag{2.4}$$

is then same for all the orbitals. The use of only the Hartree term as a self-consistent single-particle potential is equivalent to neglect of correlations as well as exchange. However, because of the inclusion of the self-interaction term, the Hartree potential (2.4) goes to zero faster than $1/r$ at large distances (since the total number of electrons is equal to $N=Z$), whereas the correct single-particle potential should behave asymptotically as $-1/r$. Indeed, in an exact calculation, this behavior should now show up in the asymptotic form of the exchange part (with the self-interaction term).

In the Hartree-Slater approximation used by Herman and Skillman in their extensive atomic calculations,[12] one replaces the effective orbital-dependent exchange-potential

$$-\frac{\sum_j \delta_{\lambda_i,\lambda_j} \int d^3r' \, \frac{u_i^*(\vec{r})u_j^*(\vec{r}')u_i(\vec{r}')u_j(\vec{r})}{|\vec{r}-\vec{r}'|}}{u_i^*(\vec{r})u_i(\vec{r})} \tag{2.5}$$

for the ith orbital in Eq. (2.2) by its average over all the orbitals. In other words, Slater assumed that the effective exchange-charge densities for different orbitals are similar in many respects, and summed the numerator and the denominator in (2.5) separately over all the occupied orbitals i. Further to calculate this resulting average exchange potential, he used uniform electron gas plane-wave orbitals[13] to find its dependence on the electronic density n. One thus obtains an expression

$$(V_X[n])_{\text{electron gas}} = -3\left(\frac{3}{8\pi}\, n\right)^{1/3}, \tag{2.6}$$

and the same functional form is then taken over for the average local exchange potential in the atomic calculation, by using the *local* value of $n(\vec{r})$ in place of the uniform n. Moreover, one uses only the spherically averaged electronic charge density $\rho(r) = \langle n(\vec{r}) \rangle$ in (2.4) and (2.6). Note that the numerical factor 3 in front of the exchange potential (2.6) is a consequence of the equal weighting given to all the occupied orbitals i, while averaging (2.5). In fact, based on total energy considerations and on the Thomas-Fermi-Dirac equation, one finds that a factor of 2 instead of 3 in the expression (2.6) may be more appropriate.[14]

Explicitly, let us denote the normalized atomic orbitals by

$$\begin{aligned}\phi_i(\vec{r},\vec{\sigma}) &= u_i(\vec{r})\chi_{\lambda_i}(\vec{\sigma}) \\ &= Y_{l_i m_i}(\hat{r})\chi_{\lambda_i}(\vec{\sigma})P_{n_i l_i}(r)/r\,,\end{aligned} \tag{2.7}$$

where Y_{lm}'s are spherical harmonics of orbital angular momentum l. In the Hartree-Slater local-density approximation, the self-consistent radial equations are of the form

$$\left(-\frac{1}{2}\frac{d^2}{dr^2} + \frac{l_i(l_i+1)}{2r^2} + V_{\text{HS}}(r) - \epsilon_{n_i l_i}\right) P_{n_i l_i}(r) = 0\,. \tag{2.8}$$

Here, the Hartree-Slater potential is

$$V_{\text{HS}}(r) = -\frac{Z}{r} + \sum_{j\,(\text{occ})} y_0(n_j l_j, n_j l_j \,|\, r) - 3\left(\frac{3}{8\pi}\,\rho(r)\right)^{1/3}, \tag{2.9}$$

where the spherically averaged charge density

$$\rho(r) = \sum_{j\,(\text{occ})} |P_{n_j l_j}(r)|^2/4\pi r^2\,, \tag{2.10}$$

and where the multipole potential function is

$$y_\lambda(nl, n'l' \,|\, r) \equiv \frac{1}{r^{\lambda+1}} \int_0^r dr' (r')^\lambda P_{nl}(r') P_{n'l'}(r') + r^\lambda \int_r^\infty dr' \, \frac{P_{nl}(r')P_{n'l'}(r')}{(r')^{\lambda+1}}\,, \tag{2.11}$$

with the normalization integrals

$$\int_0^\infty dr\, |P_{nl}(r)|^2 = 1, \quad \int d\hat{r}\, |Y_{lm}(\hat{r})|^2 = 1\,. \tag{2.12}$$

It should be noted here that the local-density approximation used in (2.9) for the exchange potential (with the self-interaction term) is inappropriate at large distances, since in this approximation the exchange potential goes exponentially to zero asymptotically instead of behaving as $-1/r$.

As already mentioned, the Hartree-Slater potential is a local-density approximation to the simple Hartree-Fock theory, which, except for taking account of the Pauli principle, completely neglects electronic correlations. In the spirit of the local-density approximation just discussed, it is possible to go beyond the simple Hartree-Fock theory and include a local correlation potential in addition to the exchange potential. Based on the density-functional theory[15] of Hohenberg, Kohn, and Sham, which is a powerful generalization of the Thomas-Fermi theory, one can obtain a simple expression for the exchange-correlation potential in the slowly varying density approximation for the interacting electrons in the external potential $-Z/r$. In such a case, the functional form of the exchange-correlation potential is given by

$$V_{\text{xc}}[n(\vec{r})] = \frac{\delta E_{\text{xc}}[n]}{\delta n(\vec{r})} \cong \mu_{\text{xc}} = \frac{d}{dn}\,[n\epsilon_{\text{xc}}(n)]\,, \tag{2.13}$$

where ϵ_{xc} is the *exchange plus correlation energy* (total energy minus the kinetic energy) *per electron of the uniform electron gas* with density n, μ_{xc} is the exchange-correlation part of the chemical potential, and the functional $E_{\text{xc}}[n]$ is the exchange-correlation part of the total energy functional defined by

$$E[n] = T_0[n] - Z\int \frac{n(\vec{r})}{r}\, d^3r + \tfrac{1}{2}\iint \frac{n(\vec{r})n(\vec{r}')}{|\vec{r}-\vec{r}'|}\, d^3r\, d^3r' + E_{\text{xc}}[n]\,. \tag{2.14}$$

Here, $T_0[n]$ is the functional for the kinetic energy of a noninteracting system with density n. Note that the corresponding second and third terms of (2.14) in the case of an uniform electron gas (with

uniform positive background) are absent because of an exact cancellation, but in our atomic case the functional derivative of these terms in (2.14) with respect to $n(\vec{r})$ gives back the Hartree potential (2.4). Indeed, in (2.13) if we only put the well known expression $\epsilon_x = -(3/4\pi)(3\pi^2 n)^{1/3}$ for the exchange energy per electron of a uniform electron gas, instead of the complete per electron exchange-correlation energy ϵ_{xc}, we recover the Slater form (2.6) for the exchange potential, except for a prefactor 2 instead of 3. This difference has already been mentioned earlier.

From a detailed numerical description of the approximately known density variation of the per-electron exchange-correlation energy ϵ_{xc} for the uniform electron gas, Hedin and Lundqvist proposed to use[10]

$$V_{xc}(r) \cong \mu_{xc}(r) = -3\left(\frac{3}{8\pi}\rho(r)\right)^{1/3}\alpha(r_s(r))\,, \qquad (2.15)$$

$$\alpha(r_s) = \tfrac{2}{3} + 0.515\,643\,6\left(\frac{r_s}{21}\right)\ln\left(1+\frac{21}{r_s}\right), \qquad (2.16a)$$

$$r_s(r) = [3/4\pi\rho(r)]^{1/3}\,, \qquad (2.16b)$$

instead of the exchange potential (last term in 2.9) used by Slater. Thus, in the Hedin-Lundqvist approximation, the self-consistent, local, single-particle potential to be used in (2.8) in place of V_{HS} is given by

$$V_{HL}(r) = -\frac{Z}{r} + \sum_{j\,(\mathrm{occ})} y_0(n_j l_j, n_j l_j | r) - 3\left(\frac{3}{8\pi}\rho(r)\right)^{1/3}\alpha(r_s(r))\,, \qquad (2.17)$$

where functions y_0 and α are defined by Eqs. (2.11) and (2.16), respectively.

As in the Hartree-Slater approximation, the local exchange-correlation potential in (2.17) again goes to zero exponentially at large r, since the electronic density decays exponentially far from the core. Since at large r, $y_0(nl, nl|r)$ behaves as $1/r$, this implies that the total single-particle potential $V_{HL}(r)$ goes to zero exponentially, instead of the correct asymptotic form $-1/r$. The error, of course, arises because of including the self-interaction terms (the same term with opposite signs) in the Hartree and the exchange-correlation potentials, which at large distances go over exactly to $1/r$ and $-1/r$, respectively; and then using an approximate form for the exchange-correlation potential which violates this cancellation.

It cannot be overemphasized that for the calculation of the binding energies of highly excited Rydberg states, it is absolutely essential that the large-distance behavior of the single-particle potential be as accurate as possible. This is in contrast to ground-state calculations, where the exact large-distance behavior is not so important. In view of this, instead of using (2.17), we omit the self-interaction terms ($i=j$ terms) in both the Hartree and exchange-correlation potentials, before making the simplifying local-density approximation.[11] Although this makes both the Hartree and the exchange-correlation potential different for different orbitals, these are still local potentials with correct behavior at large distances.

Explicitly, in our calculations, for any atom under consideration, with a given single electronic configuration $\{\nu\}$ of occupied orbitals, we first obtain the bound-state radial functions $P^{(\nu)}_{n_i l_i}(r)$, the single-particle energies $\epsilon^{(\nu)}_{n_i l_i}$, and the potentials $V^{(\nu)}_{SCF}(i|r)$ by solving self-consistently the set of equations

$$\left(-\frac{1}{2}\frac{d^2}{dr^2} + \frac{l_i(l_i+1)}{2r^2} + V^{(\nu)}_{SCF}(i|r) - \epsilon^{(\nu)}_{n_i l_i}\right)P^{(\nu)}_{n_i l_i}(r) = 0 \qquad (2.18)$$

for each of the occupied orbitals i. Here, the self-consistent potential for the ith orbital (denoted by $n_i l_i$) is defined by

$$V^{(\nu)}_{SCF}(i|r) = -\frac{Z}{r} + \sum_{j\neq i\,(\mathrm{occ})} y_0(n_j l_j, n_j, l_j|r) - 3\left(\frac{3\rho(i|r)}{8\pi}\right)^{1/3}\alpha(r_{si}(r))\,, \qquad (2.19)$$

where

$$\rho(i|r) = \sum_{j\neq i\,(\mathrm{occ})} |P_{n_j l_j}(r)|^2/4\pi r^2\,, \qquad (2.20)$$

$$r_{si}(r) = [3/4\pi\rho(i|r)]^{1/3}\,. \qquad (2.21)$$

For the case of spherical-charge density arising from the core electrons, the self-consistent calculation just described gives a very good description of the intrachannel potential seen by the outer electron both in the core region and at large distances. In the next section we will discuss how we use this information about the self-consistent potentials and the core orbitals in setting up the MQDT calculation for atoms with one or two electrons outside a closed shell.

III. APPROXIMATE INTRACHANNEL AND INTERCHANNEL POTENTIALS IN THE INTERIOR REGION

Having obtained the self-consistent local potentials $V^{(\nu)}_{SCF}(i|r)$ for various orbitals i in a given electron configuration ν, together with the corresponding bound-state wave functions, we

are now in a position to set up an approximate form for the potential experienced by the Rydberg electron in the interior region of the atom. For definiteness, we will restrict our discussion to only those atoms which have either one or two electrons outside a closed atomic shell. For simplicity, we do not consider the spin-orbit coupling explicitly, keeping in mind that for large quantum numbers n, the spin-orbit splittings are quite small.

A. One-electron atoms

First, let us consider the simplest case of atoms like Na and K, which in configurations of interest here contain only one electron outside a closed spherical shell. The independent bound Rydberg channels of different total orbital angular momentum L and spin S are obtained by promoting the outer s electron of the ground-state configuration to a higher s state ($ns\,^2S$ series) or a higher p state ($np\,^2P$ series), or a higher d state ($nd\,^2D$ series), etc. Since the closed shell is very tightly bound, any other channel with the same total L and S but with one of the *core electrons* in an *excited state* does not interact significantly with the Rydberg channel having an *unexcited core*. Thus, if we neglect these interactions, the problem reduces to a single-channel problem for each of the series $ns\,^2S$, $np\,^2P$, $nd\,^2D$, etc. In the spirit of the frozen-core approximation, we assume further that the potential experienced by the Rydberg electron in the interior region of the atom is approximately the same as the potential seen by the outer s electron in the ground-state configuration (i.e., the electron which is excited to become the Rydberg electron). Since the outer s electron sees only a spherical-charge density from the other electrons, the intrachannel potential in this case is

$$V_{11}(r) = V_{\mathrm{SCF}}^{(g)}(ms\,|r)\,, \tag{3.1}$$

where $V_{\mathrm{SCF}}^{(g)}(ms\,|r)$ is the self-consistent local potential introduced in the last section, for the outer ms-electron orbital in the ground-state configuration g. For the series under consideration, $m=3$ for Na, 4 for K, and so on. Note that a reduced intrachannel potential defined by

$$U_{11}(r) = -rV_{11}(r) \tag{3.2}$$

must go to Z as $r\to 0$, and to 1 as $r\to\infty$. These reduced potentials, as obtained in our self-consistent calculation of the last section, are plotted for Na and K in Fig. 1.

For each noninteracting Rydberg series, the calculation of the quantum-defect parameter μ_1

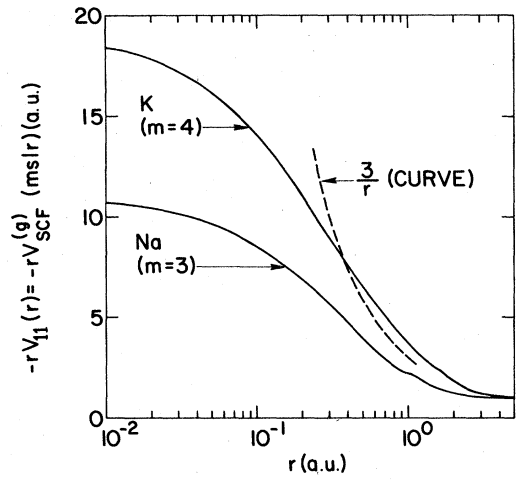

FIG. 1. A plot of the self-consistent local reduced potential $-rV_{\mathrm{SCF}}^{(g)}(ms\,|\,r)$ experienced by the outer ms electron in the ground-state configuration of Na and K. To show the crossing of the repulsive d state ($l=2$) centrifugal potential $3/r^2$ (in a.u.) with $-V_{\mathrm{SCF}}^{(g)}$ of K, the curve $3/r$ has also been plotted.

then proceeds by solving the radial Schrödinger equation

$$\left(-\frac{1}{2}\frac{d^2}{dr^2} + \frac{l_1(l_1+1)}{2r^2} + V_{11}(r) - \epsilon_1\right)F_1(r) = 0 \tag{3.3}$$

for the Rydberg electron with orbital angular momentum l_1, with the only boundary condition

$$[r^{-l_1-1}F_1(r)]\underset{r\to 0}{\to}\text{const} \tag{3.4}$$

at the origin. Here, ϵ_1 is the difference[2] $E(N) - E_1(N-1)$ of the total energies of the N-electron atom and the corresponding $(N-1)$-electron atom with only the core electrons. In other words,

$$\epsilon_1 = \epsilon - I_1\,, \tag{3.5}$$

where ϵ is the experimentally measured excitation energy of the Rydberg electron from the ground state, and I_1 is the ionization energy for the series under consideration. In our special case, I_1 is the same for all the series being investigated in a given "one-electron" atom.

In the exterior region where $V_{11}(r)$ becomes Coulombic, the solution of (3.3) can be written as

$$F_1(r) = B_1[f_1(r)\cos\pi\mu_1 - g_1(r)\sin\pi\mu_1]\,, \tag{3.6}$$

where f_1 and g_1 are Fano's regular and irregular Coulomb functions,[4] respectively, of energy $\epsilon_1 = \epsilon - I_1$ and angular momentum l_1, and where B_1 and the quantum-defect parameter $\mu_1(\epsilon)$ are independent of r. Together with the known asymptotic forms for f_1 and g_1, the requirement that, for bound states $F_1(r)$ should decay ex-

ponentially at large distances then leads to the condition

$$\sin\pi(\nu_1+\mu_1)=0,\ \epsilon_1\equiv-\frac{1}{2\nu_1^2}\ . \tag{3.7}$$

In other words, bound-state energies are determined by

$$\nu_1=n-\mu_1(\epsilon),\quad n=\text{integer}\ , \tag{3.8}$$

i.e.,

$$\epsilon_1=\epsilon-I_1=-\frac{1}{2[n-\mu_1(\epsilon)]^2}\ . \tag{3.9}$$

We will present the results of our calculations of $\mu_1(\epsilon)$ for such atoms in the next section.

B. Two-electron atoms

For two electrons outside a closed shell, it is no longer possible to neglect interchannel interactions in general. For example, in Ca, the Rydberg channels $4s\,np\,^1P$ and $3\,dnp\,^1P$ interact quite strongly. In this case, in the first channel ($4snp\,^1P$) a single $4s$ electron of the ground-state configuration is excited to a Rydberg state np, whereas in the second channel ($3dnp\,^1P$) both $4s$ electrons are excited so that the core configuration has an electron in $3d$ instead of $4s$ and the Rydberg electron is in an np state. This implies that for these two channels the major part of the intrachannel potentials, which arises from spherically averaged direct- and exchange-correlation charge densities of each of the cores, can be obtained in our frozen-core approximation by calculating the self-consistent local potentials $V_{\rm SCF}^{(4s,4s)}(4s\,|r)$ and $V_{\rm SCF}^{(3d,4s)}(4s\,|r)$, experienced by the outer $4s$ electron, with the configurations outside the closed shell specified by $4s^2$ and $3d4s$, respectively. Similar calculations can be done for other alkaline-earth atoms, with obvious modifications. For channel 1, we plot the resulting potentials in Fig. 2, in the form $-rV_{\rm SCF}^{(ms,\,ms)}(ms\,|r)$ for Mg, Ca, Sr, and Ba. To show how the self-consistent potential for the second channel differs from that of the first channel, the differences $-r[V_{\rm SCF}^{(m-1d,\,ms)}(ms\,|r)-V_{\rm SCF}^{(ms,\,ms)}(ms\,|r)]$ are plotted in Fig. 3 for Ca, Sr, and Ba. Although these differences are small, it is crucial to retain them in our calculations. Note that the additional intrachannel interaction term for the second channel [having a nonspherical core charge density due to the $(m-1)d$ electron] and the interchannel interaction are still to be found. It is also interesting to note in Fig. 3 that the curves never fall with respect to each other in simple order of increasing Z.

To be able to estimate the magnitudes of additional intrachannel potentials beyond $V_{\rm SCF}^{(\nu)}$ and the couplings between the various channels, we treat the electron-electron interactions in two stages. The two electrons (valence and Rydberg) outside the closed shell are assumed to move in an effective central potential $V_{\rm eff}(r)$ representing the potential due to the nucleus and all the

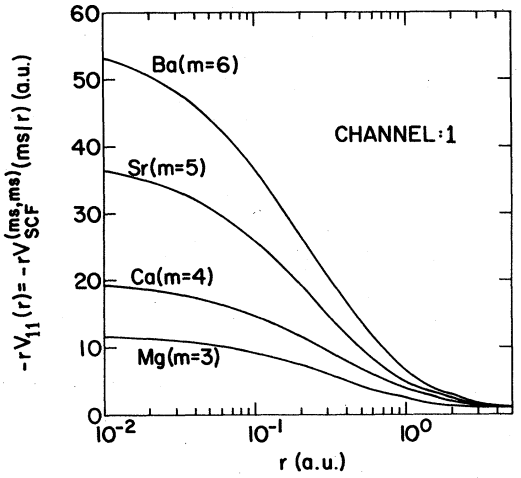

FIG. 2. The self-consistent local reduced potential $-rV_{\rm SCF}^{(ms,\,ms)}(ms\,|\,r)$ for the outer ms electron in the ground-state configuration (channel 1) is plotted for Mg ($m=3$), Ca ($m=4$), Sr ($m=5$), and Ba ($m=6$). At large distances, the reduced potential goes to 1, whereas for $r\to0$, it goes to the corresponding atomic number Z. A slight bump at r in the range 1–3 (a.u.) in each curve is real.

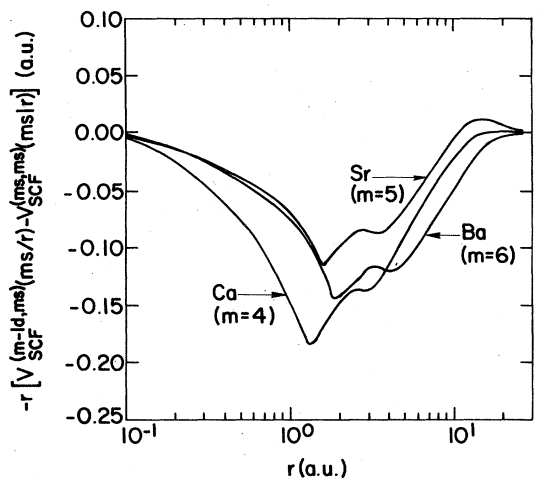

FIG. 3. The difference between the self-consistent local reduced potential $-rV_{\rm SCF}^{(m-1d,\,ms)}(ms\,|\,r)$ for the outer ms electron in channel 2 and $-rV_{\rm SCF}^{(ms,\,ms)}(ms\,|\,r)$ in channel 1 is plotted for Ca ($m=4$), Sr ($m=5$), and Ba ($m=6$). Oscillations reflecting average spatial variations of the exchange-correlation charge densities are real.

interacting electrons within the closed-shell configuration $\{c\}$. The Coulomb interaction between the outer two electrons is, however, treated explicitly. The two-electron Schrödinger equation for the outer electrons is thus given by

$$\left(-\tfrac{1}{2}\nabla_1^2+V_{eff}(r_1)-\tfrac{1}{2}\nabla_2^2+V_{eff}(r_2)+\frac{1}{|\vec{r}_1-\vec{r}_2|}\right)\Psi(1,2)=E\Psi(1,2), \quad (3.10)$$

where the labels 1 and 2 refer to the coordinates of the valence and Rydberg electrons, respectively. Since we have neglected the spin-orbit coupling, the total orbital angular momentum quantum numbers L, M_L and the total spin quantum numbers S, M_S are separately good quantum numbers. Here, $\vec{L}=\vec{l}_1+\vec{l}_2$, $\vec{S}=\vec{\sigma}_1+\vec{\sigma}_2$, where $\vec{l}_1, \vec{l}_2$ are orbital and $\vec{\sigma}_1, \vec{\sigma}_2$ are spin angular momenta of the two electrons under consideration. Thus, different channels with different L, M_L, S, M_S, do not interact, and for a given L, M_L, S, M_S, one may expand $\Psi(1,2)$ as

$$\Psi_{L,M_L,S,M_S}(1,2)=\frac{1}{\sqrt{2}}\sum_q\sum_{m_1,m_2}\sum_{\lambda_1,\lambda_2}[C(l_{1_q}l_{2_q}L;m_1m_2M_L)C(\tfrac{1}{2}\tfrac{1}{2}S;\lambda_1\lambda_2M_S)Y_{l_{1_q}m_1}(\hat{r}_1)P_{n_{1_q}l_{1_q}}(r_1)r_1^{-1}\chi_{\lambda_1}(\hat{\sigma}_1)$$
$$\times Y_{l_{2_q}m_2}(\hat{r}_2)F_q(r_2)r_2^{-1}\chi_{\lambda_2}(\hat{\sigma}_2)-(2\leftrightarrow 1)]$$
$$\equiv\frac{1}{\sqrt{2}}\sum_q[\Phi_q(LM_LSM_S\,|1,\hat{r}_2\hat{\sigma}_2)F_q(r_2)r_2^{-1}-(2\leftrightarrow 1)], \quad (3.11)$$

where q is the channel index (corresponding to different set of quantum numbers n_1, l_1, l_2) and the C's are Clebsch-Gordan coefficients. Note that $P_{n_{1_q}l_{1_q}}(r_1)$ is the bound-state normalized radial wave function of the valence electron moving in the effective potential $V_{eff}(r)$, whereas F_q is the unnormalized, and as yet arbitrary, function for the Rydberg electron in channel q.

The substitution of the expansion (3.11) in (3.10), multiplication of both sides of the resulting equation by $\Phi_q(LM_LSM_S\,|1,\hat{r}_2\hat{\sigma}_2)$, and subsequent integration over $1,\hat{r}_2,\hat{\sigma}_2$ lead to coupled equations satisfied by the function $F_q(r_2)$ for the Rydberg electron. The angular integrations are simplified considerably in this calculation, if we use the multipole expansion

$$\frac{1}{|\vec{r}_1-\vec{r}_2|}=\sum_{\lambda=0}^{\infty}\frac{r_<^{\lambda}}{r_>^{\lambda+1}}P_\lambda(\cos\theta_{12}) \quad (3.12)$$

and introduce coefficients f_λ for the matrix element

$$f_\lambda(l_1l_2,l_1'l_2'\,|L)=\langle l_1l_2LM_L\,|P_\lambda(\cos\theta_{12})\,|l_1'l_2'LM_L\rangle \quad (3.13)$$

in the coupled angular momentum scheme, where the total angular momentum wave function

$$|l_1l_2LM_L\rangle=\sum_{m_1,m_2}C(l_1l_2L;m_1m_2M_L)\,Y_{l_1m_1}(\hat{r}_1)\,Y_{l_2m_2}(\hat{r}_2). \quad (3.14)$$

The coefficients f_λ are related[16] to Wigner's $6j$ and $3j$ symbols, and have already been tabulated by Percival and Seaton.[17] The resulting coupled equations for $F_q(r)$ can be written as

$$\left(-\frac{1}{2}\frac{d^2}{dr^2}+\frac{l_{2_q}(l_{2_q}+1)}{2r^2}+\tilde{V}_{qq}(r)-\tilde{W}_{qq}(r)-\epsilon_q\right)F_q(r)$$
$$=-\sum_{q'\neq q}[\tilde{V}_{qq'}(r)-\tilde{W}_{qq'}(r)]F_{q'}(r), \quad (3.15)$$

where the direct-potential function

$$\tilde{V}_{qq'}(r)=V_{eff}(r)\delta_{qq'}$$
$$+\sum_\lambda y_\lambda(n_{1_q}l_{1_q},n_{1_{q'}}l_{1_{q'}}\,|r)f_\lambda(l_{1_q}l_{2_q},l_{1_{q'}}l_{2_{q'}}\,|L), \quad (3.16)$$

and the nonlocal exchange-potential function

$$\tilde{W}_{qq'}F_{q'}(r)=(-1)^{1-S}\sum_\lambda(-1)^{l_1+l_2-L}f_\lambda(l_{1_q}l_{2_q},l_{2_{q'}}l_{1_{q'}}\,|L)[\delta_{\lambda,0}\Delta(P_{n_{1_q}l_{1_q}},F_{q'})+y_\lambda(n_{1_q}l_{1_q},F_{q'}\,|r)]P_{n_{1_{q'}}l_{1_{q'}}}(r), \quad (3.17)$$

and where

$$\Delta(A,B)\equiv\int_0^\infty dr\,A^*(r)B(r). \quad (3.18)$$

Since, by inspection,

$$f_0(l_1l_2,l_1'l_2'\,|L)=\delta_{l_1l_1'}\delta_{l_2l_2'}, \quad (3.19)$$

note that the $\lambda=0$ term in the direct intrachannel potential $\tilde{V}_{qq}(r)$, corresponding to the spherical part of the core-charge density, is exactly equal to $y_0(n_{1_q}l_{1_q}, n_{1_q}l_{1_q}|r)$. This is just the contribution from the spherically averaged valence-electron charge density outside the closed shell in our Hartree term in (2.19), which must be added to $V_{\text{eff}}(r)$ coming from the closed-shell electron configuration $\{c\}$ only. However, $\lambda\neq 0$ terms in $\tilde{V}_{qq}$ of (3.16) are additional terms in the intrachannel potential due to the nonspherical part of the core-charge density which were ignored in our self-consistent calculation of the last section. Similar correction terms also occur in the intrachannel exchange interaction $\tilde{W}_{qq}F_q(r)$. However, because of the fact that the exchange-correlation potential has already been approximated considerably, while using our self-consistent local-density approximation in Sec. II, it is more appropriate to ignore such small corrections in the exchange term. Thus, in terms of our self-consistent potential $V_{\text{SCF}}^{(\nu)}$ of Sec. II, we can take the total intrachannel potential to be approximately represented by

$$(\tilde{V}_{qq}-\tilde{W}_{qq})F_q(r)\cong\left(V_{\text{SCF}}^{\{c\},n_{1_q}l_{1_q},i}(i|r)+\sum_{\lambda\neq 0}y_\lambda(n_{1_q}l_{1_q};n_{1_q}l_{1_q}|r)f_\lambda(l_{1_q}l_{2_q},l_{1_q}l_{2_q}|L)\right)F_q(r)\equiv V_{qq}(r)F_q(r)\,, \tag{3.20}$$

where i is the outer electron in the ground-state configuration, $\{c\}$ refers to the closed-shell ground-state configuration, and $n_{1_q}l_{1_q}$ refers to the configuration of the valence electron in the channel q. The right-hand side of Eq. (3.15), of course, represents interchannel interaction. This, as well as the second term in (3.20), can be obtained immediately in terms of the bound-state wave functions $P_{n_{1_q}l_{1_q}}(r)$ for the valence electron in each of the channel q, calculated in our self-consistent procedure of the last section.

Many Rydberg series of the alkaline earth may be described by two interacting channels. As an example, consider the interacting series $ms\,np\,^{2S+1}P$ (channel 1) and $(m-1)d\,np\,^{2S+1}P$ (channel 2). For Ca, Sr, and Ba, as already stated, $m=4$, 5, and 6, respectively. Here, one can have the total spin $S=0$ (singlet) or 1 (triplet). For Ca and Sr, only one member of the $(m-1)dnp$ channel is bound, but in Ba there are three bound members of this channel. With $l_{21}=l_{22}=1$, $L=1$, the coupled equations (3.15), in our approximation (3.20) for these two channels, then reduce to

$$\left(-\frac{1}{2}\frac{d^2}{dr^2}+\frac{1}{r^2}+V_{11}(r)-(\epsilon-I_1)\right)F_1(r)=\tfrac{1}{5}\sqrt{2}\,y_2(ms,m-1d|r)F_2(r)-(-1)^{1-S}\tfrac{1}{3}\sqrt{2}\,y_1(ms,F_1|r)P_{m-1d}(r)\,, \tag{3.21}$$

$$\left(-\frac{1}{2}\frac{d^2}{dr^2}+\frac{1}{r^2}+V_{22}(r)-(\epsilon-I_2)\right)F_2(r)=\tfrac{1}{5}\sqrt{2}y_2(m-1d,ms|r)F_1(r)-(-1)^{1-S}\tfrac{1}{3}\sqrt{2}y_1(m-1d,F_1|r)P_{ms}(r), \tag{3.22}$$

where the local intrachannel potentials V_{11} and V_{22} are given by

$$V_{11}(r)=V_{\text{SCF}}^{(ms,ms)}(ms|r)\,, \tag{3.23}$$

$$V_{22}(r)=V_{\text{SCF}}^{(m-1d,ms)}(ms|r)+\tfrac{1}{5}y_2(m-1d,m-1d|r)\,, \tag{3.24}$$

for the two channels. Here, I_q is the ionization energy (in a.u.) for the channel q, and for brevity we have omitted to write the common closed-shell configuration $\{c\}$ while specifying the full configurations for V_{SCF}.

Note that at sufficiently large distances, y_2 goes to zero as $1/r^3$ and the interchannel exchange term goes to zero exponentially. Thus at large distances the channels are uncoupled [i.e., the right-hand sides of (3.21) and (3.22) are negligible], and for each channel the potential is asymptotically equal to $-1/r$. Therefore, in the outside region, Rydberg functions F_1 and F_2 are again linear combinations of Coulomb functions, and one can write

$$F_q(r)=f_q(r)A_q-g_q(r)\sum_{q'}(\tan\pi\mu)_{qq'}A_{q'}\,, \tag{3.25}$$

where f_q's (g_q's) are regular (irregular) Coulomb functions of Fano[9] for the channel $q=1$ or 2, with energy $\epsilon_q=\epsilon-I_q$. Equation (3.25) *defines* a symmetric matrix μ, which is known by matching, once $F_q(r)$ and (dF_q/dr) have been calculated from (3.21) and (3.22) in the inside region.

After obtaining the symmetric matrix μ, one can diagonalize it by a rotation matrix U:

$$U=\begin{pmatrix}\cos\theta & -\sin\theta\\ \sin\theta & \cos\theta\end{pmatrix},$$

$$U^{-1}(\tan\pi\mu)U=\tan\pi\bar{\mu}=\begin{pmatrix}\tan\pi\mu_1 & 0\\ 0 & \tan\pi\mu_2\end{pmatrix}, \tag{3.26}$$

where μ_1 and μ_2 are eigenquantum defects and θ

is the channel-interaction angle. In the absence of channel interaction θ is zero, and $\mu_1(\epsilon)$ and $\mu_2(\epsilon)$ then just represent the usual quantum defects described in Sec. III A (when the corresponding channel is closed, i.e., when $\epsilon_q<0$), or the usual ion-electron scattering phase shifts in units of π (when the corresponding channel is open, i.e., when $\epsilon_q>0$). In the general case, when both the channels are closed, the bound-state conditions on $F_q(r)$ at $r\to\infty$ then lead to the relation[3]

$$\det\begin{pmatrix}\cos\theta\sin\pi(\nu_1+\mu_1) & -\sin\theta\sin\pi(\nu_1+\mu_2)\\ \sin\theta\sin\pi(\nu_2+\mu_1) & \cos\theta\cos\pi(\nu_2+\mu_2)\end{pmatrix}=0\,, \tag{3.27}$$

where

$$-\frac{1}{2\nu_1^2}\equiv\epsilon_1=\epsilon-I_1\,,\quad -\frac{1}{2\nu_2^2}\equiv\epsilon_2=\epsilon-I_2\,. \tag{3.28}$$

Bound-state energies are found from the simultaneous solution of (3.27), which can be written $\nu_1=$function (ν_2), with the relation between ν_1 and ν_2 which comes from eliminating ϵ in the two equations in (3.28), namely,

$$\frac{1}{2\nu_1^2}=\frac{1}{2\nu_2^2}-(I_2-I_1)\,. \tag{3.29}$$

The determination of bound-state energies from the simultaneous solution of a trigonometric and an algebraic equation is characteristic of MQDT. Equation (3.27) leads essentially to the normalization of the two-electron radial functions, and this normalization is carried out only *after* the channel interactions have been taken into account by the parameters μ_1, μ_2, and θ.

There is a useful graphical representation of the solutions to (3.27) and (3.29). The first equation is periodic in both ν_1 and ν_2 as independent variables, and so, as is done in the so-called reduced-zone scheme in solid-state calculations, the entire functional variation of (3.27) can be represented in a unit square of the ν_1,ν_2 plane. Equation (3.29) is not periodic, however. It represents ν_1 as a monotonically varying function of ν_2, starting at the origin and going to a vertical asymptote, $\nu_1\to\infty$, when $\nu_2(\max)=\{[2(I_2-I_1)]^{1/2}\}^{-1}$, assuming $I_2>I_1$. When this function is reflected back into the unit (ν_1,ν_2) square, it has infinitely many branches, crowding up to the vertical tangent at $\nu_2(\max)$. By convention, (3.27) and (3.29) are each solved for $-\nu_1$ as functions of ν_2 and plotted on the unit square to make a so-called Lu-Fano plot, as shown in Fig. 4 for a typical case. The intersections (circled) give the bound-state energies. Explicit evaluation of μ_1, μ_2, and θ for the two-channel problem in Ca, Sr, and Ba will be described in Sec. IV.

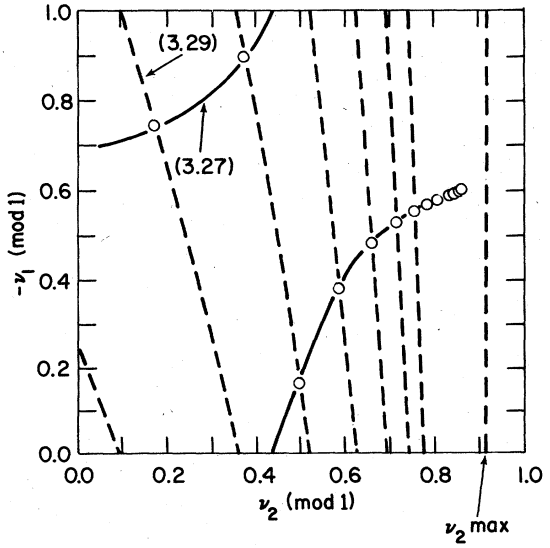

FIG. 4. A typical plot of curves $-\nu_1(\nu_2)$ representing Eqs. (3.27) and (3.29) in a reduced-zone scheme. The intersections (circled) of these curves in this Lu-Fano plot determine bound-state energies in the interacting two-channel case.

IV. NUMERICAL CALCULATION OF QUANTUM-DEFECT PARAMETERS

In Sec. III, we have presented our method of constructing explicitly the intrachannel and interchannel interactions for various Rydberg series in one-electron as well as two-electron atoms. For Rydberg series $ns\,^2S$, $np\,^2P$, or $nd\,^2D$ in atoms like Na and K, the calculation involves only a single channel. This is not true for some of the Rydberg series in two-electron atoms like Ca, Sr, and Ba, where one has to introduce channel interactions to fit experimental spectra. For example, the odd parity $^1P_1$ spectra require at least two channels. We now discuss our numerical procedure for obtaining the corresponding quantum-defect parameters in both these cases, and present final results of such calculations.

For Rydberg series in atoms like Na or K, where the outermost s electron in the ground-state configuration is excited to a level in the Rydberg series of orbital angular momentum l_1, we have to solve the radial equation (3.3):

$$\left(-\frac{1}{2}\frac{d^2}{dr^2}+\frac{l_1(l_1+1)}{2r^2}+V_{11}(r)-(\epsilon-I_1)\right)F_1(r)=0 \tag{4.1}$$

for energy ϵ close to the ionization energy I_1 of the series, with

$$\lim_{r\to 0}[r^{-l_1-1}F_1(r)] = \text{const.} \tag{4.2}$$

Here, $V_{11} = V_{SCF}^{(g)}(ms\,|r)$ is the self-consistent local potential for the outermost ms electron in the ground-state configuration of the atom, as plotted in Fig. 1 for Na and K. Once the intrachannel potential $V_{11}(r)$ is known from our self-consistent calculation, the differential equation (4.1) is solved numerically, starting very close to the origin, where the initial values satisfy the relation (4.2). The logarithmic derivative $F_1'(r)/F_1(r)$ of the resulting solution is then matched to the corresponding derivative of the radial Coulomb functions [to be defined explicitly in (4.4)] at the matching radius r_0:

$$\frac{F_1'(r_0)}{F_1(r_0)} = \frac{f_1'(r_0) - g_1'(r_0)\tan\pi\mu_1(\epsilon)}{f_1(r_0) - g_1(r_0)\tan\pi\mu_1(\epsilon)} \tag{4.3}$$

for the same energy ϵ. This determines the quantum-defect parameter $\mu_1(\epsilon)$ of the series under consideration for the chosen energy ϵ. Note that if r_0 is chosen much smaller than the radius beyond which the potential $V_{11}(r)$ behaves approximately as $-1/r$, μ_1 will not be independent of r_0. In fact, to keep track of the complete variation of the quantum-defect parameter $\mu_1(\epsilon)$ with the matching radius r_0, thereby obtaining even its *integer part* instead of μ_1 (modulo 1), we match the logarithmic derivative $F_1'(r)/F_1(r)$, via Eq. (4.3), at different r_0, starting close to the origin. Each time $\arg(\tan\pi\mu_1)$ changes by π, unity is added to μ_1. The numerical integration of (4.1) then extends in r just far enough for V_{11} to behave as $-1/r$, so that $\mu_1(\epsilon)$ in (4.3) finally becomes *numerically* independent of the matching radius r_0.

Explicitly, Fano's Coulomb functions f_1 and g_1 are calculated for any value of r by following Curtis[9], i.e., by first calculating the functions $P_L(a,x)$ and $Q_L(a,x)$ introduced by him. For the energy parameter $\epsilon_1 = \epsilon - I_1 < 0$, these are related by normalization factors given by

$$f_1(r) \equiv f_{l_1}(\epsilon_1, r) = \frac{2^{l_1+1}}{\Gamma(2l_1+2)} A^{1/2}(2\epsilon_1, l_1)\, P_{l_1}(2\epsilon_1, r), \tag{4.4a}$$

$$g_1(r) \equiv g_{l_1}(\epsilon_1, r) = \frac{2^{l_1+1}}{\Gamma(2l_1+2)} A^{1/2}(2\epsilon_1, l_1)\, Q_{l_1}(2\epsilon_1, r), \tag{4.4b}$$

where

$$f_1(r)g_1'(r) - g_1(r)f_1'(r) = 2/\pi\ . \tag{4.5a}$$

$$\Gamma(2l+2) = (2l+1)!\,; A(a,1) = 1\times(1+a)\times(1+4a)\times\cdots\times(1+l^2a), \tag{4.5b}$$

and

$$\left(\frac{d^2}{dr^2} + a + \frac{2}{r} - \frac{l(l+1)}{r^2}\right)\begin{pmatrix} P_l(a,r) \\ Q_l(a,r)\end{pmatrix} = 0\ . \tag{4.6}$$

For various series in Na and K, our numerical results for the quantum-defect parameters, very close to the respective ionization limits, are shown in Table I. Experimental values for these parameters as derived from the energy levels in Moore's table[18] [using Eq. (3.9)] are also shown there for comparison. Except for the nd^2D series in K, the agreement is quite good. As discussed by Greene,[6] the crossover point of the self-consistent attractive potential $V_{11}(r)$ in K and the repulsive centrifugal potential $3/r^2$ for d states occurs approximately at $r \sim 0.5$ a.u. (see Fig. 1). Thus, the net potential for the d state in K is very small in exactly the region where an accurate calculation of $V_{11}(r)$ is most delicate. A good index of the success of further refinements to our calculation scheme will be the ability to do better on ^2D states. For Rydberg series with s and p orbitals, the potential $V_{11}(r)$ seems to be excellent.

For interacting channels $ms\,np^{2S+1}P$ (channel 1) and $(m-1)d\,np^{2S+1}P$ (channel 2) in two-electron atoms like Ca, Sr, and Ba, we have to solve the coupled equations (3.21) and (3.22). To set up these equations, we first solve the self-consistent problem defined by Eqs. (2.18)–(2.21), for these two channels separately, with configuration outside the closed shell given by ms^2 and $(m-1)dms$, respectively. This gives us not only the self-consistent potentials for the $4s$ orbital in each channel (Figs. 2 and 3), it also determines the radial bound-state functions $P_{ms}(r)$ and $P_{(m-1)d}(r)$ in these two channels. The expressions (3.23) and (3.24) for the intrachannel potentials V_{11} and V_{22}, and the definition (2.11) of the multipole function $y_\lambda(A, B|r)$ then immediately lead to the determination of both the intrachannel and interchannel interaction terms in (3.21) and (3.22).

Notice that because of the nonlocal exchange interaction in the interchannel potential, Eqs. (3.21)

TABLE I. Calculated values of quantum defects $\mu_1(I_1)$ at the ionization limit in several Rydberg series in one-electron atoms with independent channels. Measured values derived from Ref. 18 are also listed.

Z	Atom	Theory T Expt. (E)	ns^2S series	np^2P series	nd^2D series
11	Na	T	1.356	0.856	0.013
		(E)	(1.35)	(0.85)	(.01)
19	K	T	2.19	1.71	0.56
		(E)	(2.18)	(1.70)	(0.28)

and (3.22) still represent a set of integrodifferential equations. In fact, we may rewrite these in the general form

$$\left(\frac{d^2}{dr^2} - \frac{l_1(l_1+1)}{r^2} - 2V_{11}(r) + 2\epsilon_1\right) F_1(r) = 2\int dr' V_{12}(r,r') F_2(r') , \quad (4.7)$$

$$\left(\frac{d^2}{dr^2} - \frac{l_2(l_2+1)}{r^2} - 2V_{22}(r) + 2\epsilon_2\right) F_2(r) = 2\int dr' V_{21}(r,r') F_1(r') , \quad (4.8)$$

where for the interacting ^{2S+1}P channels under consideration,

$$V_{12}(r,r') = V_{21}(r',r) = -\left[\frac{\sqrt{2}}{5}\delta(r'-r)\int_0^\infty dr''\left(\frac{(r'')^2}{r^3} P_{ms}(r'')P_{m-1d}(r'')\Theta(r-r'') + \frac{r^2}{(r'')^3} P_{ms}(r'')P_{m-1d}(r'')\Theta(r''-r)\right) - (-1)^{1-S}\frac{\sqrt{2}}{3}\left(\frac{r'}{r^2} P_{ms}(r')P_{m-1d}(r)\Theta(r-r') + \frac{r}{(r')^2} P_{ms}(r')P_{m-1d}(r)\Theta(r'-r)\right)\right] , \quad (4.9)$$

with $\Theta(x)$ being the usual unit-step function

$$\Theta(x) = \begin{cases} 0, & x<0 \\ 1, & x>0 . \end{cases} \quad (4.10)$$

There are standard numerical techniques[4] for solving the set of integrodifferential equations (4.7) and (4.8). One of the methods, which we follow here is to obtain first the Green's function $g_i(r,r')$ for each of the channels $i=1,2$ which satisfy the ordinary differential equations

$$D_i g_i(r,r') \equiv \left(\frac{d^2}{dr^2} - \frac{l_i(l_i+1)}{r^2} - 2V_{ii}(r) + 2\epsilon_i\right) g_i(r,r') = \delta(r-r') . \quad (4.11)$$

In terms of the regular and irregular solutions $F_{i0}(r)$ and $G_{i0}(r)$, respectively, of the corresponding uncoupled homogeneous equations

$$D_i F_{i0}(r) = 0, \; D_i G_{i0}(r) = 0 , \quad (4.12)$$

with the chosen Wronskian condition

$$F_{i0}(r)G'_{i0}(r) - F'_{i0}(r)G_{i0}(r) = 1 , \quad (4.13)$$

The Green's function g_i is given by

$$g_i(r,r') = F_{i0}(r)G_{i0}(r')\Theta(r'-r) + F_{i0}(r')G_{i0}(r)\Theta(r-r') . \quad (4.14)$$

It should be emphasized here that the regular solution F_{i0} is similar to that obtained for the single-channel problem, satisfying the condition (4.2). The irregular solution is obtained by imposing the condition that at small r, $r^{l_i}G_{i0}(r)$ $\to$ const, with the constant so chosen that the Wronskian condition (4.13) is satisfied exactly. In fact, since for very small r, $V_{ii}(r) \to -Z/r$, to find F_{i0} and G_{i0} we start our numerical procedure close to the origin with the known regular and irregular Coulomb functions for the potential $-Z/r$, apart from adjusting a multiplicative constant for G_{i0} to satisfy the Wronskian condition (4.13).

Once the Green's function $g_i(r,r')$ for each channel is calculated, the general solutions of Eqs. (4.7) and (4.8) can be obtained by solving the coupled integral equations

$$F_1(r) = F_{10}(r)d_1 + \int_0^{r_0} dr' \int_0^{r_0} dr'' g_1(r,r') \times 2V_{12}(r',r'')F_2(r'') , \quad (4.15)$$

$$F_2(r) = F_{20}(r)d_2 + \int_0^{r_0} dr' \int_0^{r_0} dr'' g_2(r,r') \times 2V_{21}(r',r'')F_1(r'') , \quad (4.16)$$

by iteration. Here, d_1 and d_2 are arbitrary constants, and r_0 is the cutoff radius beyond which the interchannel interaction is vanishing small and both intrachannel potentials start behaving as $-1/r$. In the first iteration, one replaces $F_2(r)$ and $F_1(r)$ on the right-hand sides of these coupled equations by their uncoupled values $F_{20}(r)d_2$ and $F_{10}(r)d_1$, respectively. Thus, to the first approximation, at the matching radius r_0, one finds (in matrix notation)

$$\begin{pmatrix} F_1(r_0) \\ F_2(r_0) \end{pmatrix} \cong \begin{pmatrix} F_{10}(r_0) & G_{10}(r_0)L_{12} \\ G_{20}(r_0)L_{21} & F_{20}(r_0) \end{pmatrix} \begin{pmatrix} d_1 \\ d_2 \end{pmatrix} , \quad (4.17)$$

where

$$L_{12} \equiv [L_{12d} - (-1)^{1-S} L_{21x}] = L_{21} , \quad (4.18)$$

TABLE II. Calculated values of quantum eigendefects $\mu_1(I_1)$ and $\mu_2(I_1)$, and their energy derivatives (in a.u.) at the ionization limit I_1, for weakly interacting triplet channels $ms\,np\,^3P$, respectively, in two-electron atoms. Measured values (Refs. 18–20), wherever available, are also listed. I_1 and I_2 are ionization energies for channels 1 and 2, respectively.

Atom	I_1 (a.u.) ms core	I_2 (a.u.) $(m-1)\,d$ core	Theory T Expt. (E)	Channel 1: $ms\,np\,^3P$ $\mu_1(I_1)$	$(d\mu_1/d\epsilon)_{I_1}$	Channel 2: $(m-1)\,dnp\,^3P$ $\mu_2(I_1)$	$(d\mu_2/d\epsilon)_{I_1}$
Mg	0.280 985 29		T	1.125	−0.52		
			(E)	(1.14)			
Ca	0.224 654 63	0.287 126 27	T	1.96	−0.72	1.81	−0.20
			(E)	(1.97)	(−0.76)	(1.84)	
Sr	0.209 282 47	0.276 242 69	T	2.88	−0.80	2.80	−0.55
			(E)	(2.90)	(−0.81)	(2.81)	
Ba	0.191 525 11	0.213 733 45	T	3.79	−1.10	3.63	−0.40
			(E)	3.81	(−1.12)	(3.70)	

$$L_{12d} = -2\int_0^{r_0} dr' \int_0^{r_0} dr'' F_{10}(r')F_{20}(r')P_{ms}(r'')P_{m-1d}(r'')\frac{\sqrt{2}}{5}\left(\frac{(r'')^2}{(r')^3}\Theta(r'-r'') + \frac{(r')^2}{(r'')^3}\Theta(r''-r')\right) \tag{4.19}$$

$$L_{12x} = -2\int_0^{r_0} dr' \int_0^{r_0} dr'' F_{10}(r')F_{20}(r')P_{ms}(r'')P_{m-1d}(r')\frac{\sqrt{2}}{3}\left(\frac{r''}{(r')^2}\Theta(r'-r'') + \frac{r'}{(r'')^2}\Theta(r''-r')\right). \tag{4.20}$$

The first term L_{12d} in Eq. (4.18) comes from the direct interchannel interaction, whereas the second term L_{12x} comes from the nonlocal exchange term in the interchannel interaction.

By examining the expressions for L_{12d} and L_{12x} given by Eqs. (4.19) and (4.20), and by actual numerical integrations of these expressions, we find that both these terms are approximately of the same order in magnitude. This explains why for the triplet channels ($S=1$), L_{12x} almost exactly cancels L_{12d} so that the total interaction parameter L_{12} is very weak, whereas for the singlet channels ($S=0$), L_{12x} adds almost equally to L_{12d}, giving a large interaction parameter. This is consistent with various experimental observations[19,20] for these channels. Although a complete treatment would involve solving the set of integrodifferential equations (4.7) and (4.8) exactly, in what follows we continue in the spirit of local-potential approximation and assume that L_{12x} is exactly equal to L_{12d} in (4.18). In other words, we assume that the effect of the nonlocal interchannel exchange term in Eqs. (4.7) and (4.8) is the same as that of the direct term for $S=0$, and that they cancel each other exactly for $S=1$.

By comparing the approximate solution (4.17)

TABLE III. Calculated values of quantum eigendefects $\mu_1(I_1)$ and $\mu_2(I_1)$, and the interaction parameter $\theta(I_1)$, at the ionization limit I_1 for strongly interacting $ms\,np\,^1P$ and $(m-1)dnp\,^1P$ channels in Ca, Sr, and Ba. Measured values (Refs. 19 and 20) are also listed. Ionization energies I_1 and I_2 are same as in Table II.

Z	Atom	Theory T Expt. (E)	$\mu_1(I_1)$	$\mu_2(I_1)$	$\theta(I_1)$
20	Ca	T	1.95	1.59	0.67
		(E)	(1.97)	(1.57)	(0.60)
38	Sr	T	2.94	2.67	0.66
		(E)	(2.89)	(2.49)	(0.61)
56	Ba	T	3.85	3.52	0.61
		(E)	(3.79)	(3.51)	(0.61)

TABLE IV. Calculated values of quantum defects $\mu_1(I_1)$, and their energy derivatives $(d\mu_1/d\epsilon)_{I_1}$ in a.u. at the ionization limit I_1, for the noninteracting triplet channels $ms\,ns\,^3S$ and $ms\,nd\,^3D$, in two-electron atoms. Measured values (Refs. 18 and 19), wherever available, are also listed. The ionization energy I_1 is same as in Table II.

Atom	Theory T Expt. (E)	$ms\,ns\,^3S$ series $\mu_1(I_1)$	$(d\mu_1/d\epsilon)_{I_1}$	$ms\,nd\,^3D$ series $\mu_1(I_1)$	$(d\mu_1 d\epsilon)_{I_1}$
Mg	T	1.604	−0.44	0.196	−0.24
	(E)	(1.63)		(0.18)	
Ca	T	2.42	−0.52	1.01	−0.72
	(E)	(2.45)		(0.87)	
Sr	T	3.34	−0.64	1.90	−0.96
	(E)	(3.37)		(1.77)	
Ba	T	4.24	−0.76	2.89	−1.28
	(E)	(4.25)		(2.85)	

TABLE V. Some typical comparisons of our calculated excitation energies of Rydberg states with their observed values (Refs. 18–20) (measured from the ground-state energy of the respective atoms).

Atom	Level	Calculated energy (in cm^{-1})	Observed energy (in cm^{-1})	I_1 (in cm^{-1})	I_2 (in cm^{-1})
Ca	$4s60p:^3P$	49 273.41	49 273.37 ± .03	49 305.99	63 016.93
	$4s14p:^3P$	48 548.38	48 548.30		
	$4s7p:^3P$	44 954.65	44 957.65($^3P_1$)		
	$3d4p:^3P$	39 691	39 335($^3P_1$)		
	$4s14p:^1P_1$	48 565.5	48 567		
	$3d4p:^1P_1$	43 602	43 937		
Ba	$5d6p:^1P_1$	27 950	28 554	42 034.9	47 709.96
	$5d7p:^1P_1$	38 465	38 500		

(and its derivative at r_0) with the corresponding (outside) Coulomb solutions (3.25) at r_0, we then obtain the quantum-defect matrix μ, for a given value of ϵ, simply by solving the resulting simultaneous linear (matrix) equations. The input values of $\epsilon_1 = \epsilon - I_1$ and $\epsilon_2 = \epsilon - I_2$ are inserted in our equations by using experimental values I_1 and I_2 for the two channels (averaged over spin-orbit splitting, if any; see Table II). The matrix μ is then diagonalized by using the rotation matrix U:

$$U = \begin{pmatrix} \cos\theta & -\sin\theta \\ \sin\theta & \cos\theta \end{pmatrix}, \quad U^{-1}\mu U = \begin{pmatrix} \mu_1 & 0 \\ 0 & \mu_2 \end{pmatrix}. \tag{4.21}$$

As already discussed, the eigendefect parameters $\mu_1(\epsilon)$ and $\mu_2(\epsilon)$ and the interaction angle θ determine the binding energies of the entire series of levels, via Eqs. (3.27) and (3.29).

In Tables II and III, we present our calculated values of the quantum-defect parameters for the ^3P and ^1P channels, respectively. Table II contains results for all the triplet-P channels, which are noninteracting in our approximation. For completeness, it also includes the results for the first channel ($msnp^3P$) in Mg. To show the energy dependence of each of these quantum defects near the ionization limit I_1, we write

$$\mu_i(\epsilon) \cong \mu_i(I_1) + \left(\frac{d\mu_i}{d\epsilon}\right)_I (\epsilon - I_1), \tag{4.22}$$

and tabulate the values of both $\mu_i(I_1)$ and $(d\mu_i/d\epsilon)_{I_1}$ at $\epsilon = I_1$. The corresponding available experimental results are also shown in this table. One finds good agreement between them, even though some of the experimental data have been analyzed with small amounts of channel interaction. Table III shows results for the interacting singlet-P channels. Agreement with experimental results is satisfactory, considering the numerical approximations involved in handling the full interchannel interaction.

In our approximation, the triplet channels in the two-electron atoms are taken to be noninteracting. Using the already known self-consistent potentials for the channel 1 in Mg, Ca, Sr, and Ba, we can, therefore, calculate their quantum-defect parameters for the series $ms\,ns\,^3S$, to test our procedure further. These results are shown and compared with existing experimental results in Table IV. Again, the agreement is quite good. In the same table, calculated quantum-defect parameters are shown for the $ms\,nd\,^3D$ series in these atoms.

To display directly the accuracy of our calculations of different quantum-defect parameters in predicting corresponding Rydberg-state binding energies, we show, in Table V, some typical comparisons of our theoretical values with available experimental values of these excitation energies. For the single-channel case, Eq. (3.9) is used to obtain the excitation energies $-\epsilon$, whereas for the two-channel case, Eqs. (3.27) and (3.29) are solved simultaneously to obtain $-\epsilon$ from the calculated quantum-defect parameters. As expected, for large principal quantum number n, the error is extremely small since the fractional error in predicting binding energies varies roughly as $2\Delta\mu/n$, where $\Delta\mu$ is the error in eigendefect. But even for very low-lying states (close to the ground state), the typical difference (500 cm^{-1} or 2×10^{-3} a.u.) is not bad in comparison with the accuracy of the usual ground-state atomic calculations.

V. DISCUSSION

In the preceding sections we have explicitly shown how one can construct relatively simple, local, self-consistent, intrachannel potential which may be used in reliable numerical calculations of atomic quantum-defect parameters. It

contains the usual Hartree potential seen by the outer electron due to spherically averaged charge density of the remaining core, in the channel under consideration, and the part of the Hartree potential arising from any possible nonspherical core-charge density. Moreover, it includes an approximate form of both the exchange and the correlation parts of the intrachannel potential, which is made local because of our use of an orbital-dependent local-density approximation. Owing to proper handling of self-interaction terms, our total intrachannel potential indeed behaves as $-1/r$ at sufficiently large distances from the origin. Even for almost noninteracting channels, e.g., for the triplet channel $(m-1)dnp^3P$ (channel 2) in Ca, Sr, and Ba, we find that the correlation to the intrachannel potential from the nonspherical core, although quite small, changes the corresponding quantum defect μ_2 (modulo 1) by almost 20%. It is, therefore, quite essential to include this nonspherical correction in such calculations.

We find that the Hartree-Slater potential, as modified by Herman and Skillman[12] to make it equal to $-1/r$ beyond certain r_0 from the origin, does almost as well as our intrachannel potential for noninteracting channels in one-electron atoms like Na and K. However, even for the almost noninteracting triplet channels $msnp^3P$ (channel 1), with spherical core, in two-electron atoms like Mg, Ca, Sr, and Ba, the modified Hartree-Slater potential gives errors of 10 to 30% in the corresponding quantum defects (modulo 1). It implies that for more than one-electron atoms, proper handling of self-interaction terms and inclusion of correlations are important.

For the two-electron atoms under consideration, we also showed how to obtain the interchannel interactions, by explicitly considering the interaction of the two electrons outside the closed-shell configuration. In general these interactions are nonlocal. Although, for further simplifying our numerical work we made the interchannel interaction term local in both the triplet-P and the singlet-P two-channel problems, we would like to emphasize again that it is not essential. Using the Green's-function technique described in the text, the full coupled integrodifferential equations (4.7) and (4.8) may be solved numerically without major additional complications, as long as the intrachannel potentials are local.

Our explicit numerical results for the quantum-defect parameters show that for all the noninteracting channels as well as for channel 1 ($msnp^3P$ series) in the weakly interacting triplet-P problem, not only the magnitude of the quantum defects μ_1, but the magnitude and the sign of their energy dependence are also in good agreement with the corresponding experimental numbers. The general trend of increasing energy dependence of μ_1 as we go from Mg to Ba is also reproduced quite well in our calculation, so is the fact that the energy dependence of μ_2 in the second channel $(m-1dnp^3P)$ is much weaker than the corresponding μ_1.

On the other hand, for the strongly interacting singlet-P problem we find that the eigenquantum defect μ_2 and the interaction angle θ vary with energy, most appreciably in the case of Ba ^1P. This variation of θ with ϵ was also found experimentally for Ba in Ref. 19. The calculations described here showed some energy dependence of θ on ϵ for Ca and Sr as well. This is consistent with the results of Geiger's MQDT description of Ca ^1P autoionizing resonances.[21] We have to take this energy dependence of θ into account to obtain bound-state energies (a few of which are displayed in Table V). For strongly interacting singlet-P channels the overall agreement between the calculated and experimental quantum-defect parameters is not so good, particularly for channel 2. However, we expect this to improve considerably when the coupled integrodifferential equations (4.7) and (4.8) are handled without further approximations. The interchannel interaction term we believe, is quite accurate, except for the fact that we would have to include more than two channels in our calculation (e.g., the $5dnf\,^1P$ channel in Ba) to reproduce all the fine details of the spectrum. In conclusion, we mention that our approach and the constructed potentials can also be used to obtain partial scattering phase shifts for open channels, and autoionization energies and their widths for a closed channel in the presence of another open channel.

ACKNOWLEDGMENT

We wish to thank J.F. Janak of our laboratory for helping us with a computer program for the self-consistent calculation of the singlet-particle atomic potential.

*Permanent address: Tata Institute of Fundamental Research, Bombay 400 005, India.

[1]For a recent list of references, see, e.g., J. J. Wynne and J. A. Armstrong, IBM J. Res. Dev. 23, 490 (1979).

[2]M. J. Seaton, Proc. Phys. Soc. London 88, 801 (1966); Comments At. Mol. Phys. D2, 37 (1970), and references therein.

[3]U. Fano, J. Opt. Soc. Am. 65, 979 (1975); K. T. Lu and U. Fano, Phys. Rev. A 2, 81 (1970); U. Fano, *ibid.* 2, 353 (1970).

[4]K. Smith, *The Calculation of Atomic Collision Process* (Wiley, New York, 1972); P. B. Burke and M. J. Seaton, in *Methods of Computational Physics*, edited by B. Alder, S. Fernbach, and M. Rotenberg (Academic, New York, 1971), Vol. 10.

[5]R. G. Parson and V. F. Weisskopf, Z. Phys. 202, 492 (1967); D. L. Moores, Proc. Phys. Soc. London 91, 830 (1967); N. A. Doughty, M. J. Seaton, and V. B. Shorey, J. Phys. B 1, 802 (1968); J. Dubau and J. Wells, *ibid.* 6, 1452 (1973).

[6]C. M. Lee, Phys. Rev. A 10, 584 (1974); C. H. Greene, *ibid.* 20, 656 (1979); F. H. Mies, *ibid.* 20, 1773 (1979); W. R. Johnson and C. D. Lin, *ibid.* 20, 964 (1979).

[7]For the special case of two electrons outside the closed shell, a hyperspherical coordinate approach has been used recently for Be by C. H. Greene, Phys. Rev. A 23, 661 (1981).

[8]K. C. Pandey, S. S. Jha, and J. A. Armstrong, Phys. Rev. Lett. 44, 1583 (1980).

[9]For a discussion of Coulomb functions introduced by Fano, see, e.g., C. Greene, U. Fano, and G. Strinati, Phys. Rev. A 19, 1485 (1979). For a tabulation of Coulomb functions with different normalization factors, see, A. R. Curtis, *Coulomb Wave Functions, Royal Society Mathematical Tables, Vol. 11* (University Press, Cambridge, 1964).

[10]L. Hedin and B. I. Lundqvist, J. Phys. C 4, 2064 (1971).

[11]J. P. Perdew, Chem. Phys. Lett. 64, 127 (1979); J. F. Janak (unpublished).

[12]See, F. Herman and S. Skillman, *Atomic Structure Calculations* (Prentice-Hall, Englewood Cliffs, N. J., 1963).

[13]See, e.g., J. C. Slater, *Quantum Theory of Matter* (McGraw-Hill, New York, 1968).

[14]R. Gaspar, Acta Phys. Hung. 3, 263 (1954).

[15]P. Hohenberg and W. Kohn, Phys. Rev. 136, B864 (1964); W. Kohn and L. J. Sham, *ibid.* 140, A1133 (1965); B. Y. Tong and L. J. Sham, *ibid.* 144, 1 (1966).

[16]A. R. Edmonds, *Angular Momentum in Quantum Mechanics* (Princeton University Press, Princeton, N. J., 1957), p. 114.

[17]I. C. Percival and M. J. Seaton, Proc. Cambridge Philos. Soc. 53, 654 (1957).

[18]C. E. Moore, *Atomic Energy Levels*, National Bureau of Standards Circular No. 467 (U. S. GPO, Washington, D. C., 1949, 1952, and 1958), Vols. 1–3.

[19]J. A. Armstrong, J. J. Wynne, and P. Esherick, J. Opt. Soc. Am. 69, 211 (1979); Phys. Rev. A 15, 180 (1977); P. Esherick, *ibid.* 15, 1920 (1977).

[20]C. M. Brown, S. G. Tilford, and M. Ginter, J. Opt. Soc. Am. 63, 1454 (1973); W. R. S. Garton and F. S. Tomkins, Astrophys. J. 158, 1219 (1969).

[21]J. Geiger, J. Phys. B 12, 2277 (1979).